

## Direct observation of UV-induced charge accumulation in inverted-type polymer solar cells with a TiO<sub>x</sub> layer: Microscopic elucidation of the light-soaking phenomenon

D. Son, T. Kuwabara, K. Takahashi, and K. Marumoto

Citation: [Applied Physics Letters](#) **109**, 133301 (2016); doi: 10.1063/1.4963285

View online: <http://dx.doi.org/10.1063/1.4963285>

View Table of Contents: <http://scitation.aip.org/content/aip/journal/apl/109/13?ver=pdfcov>

Published by the [AIP Publishing](#)

---

### Articles you may be interested in

[The appearance of Ti3+ states in solution-processed TiO<sub>x</sub> buffer layers in inverted organic photovoltaics](#)  
Appl. Phys. Lett. **109**, 022108 (2016); 10.1063/1.4958892

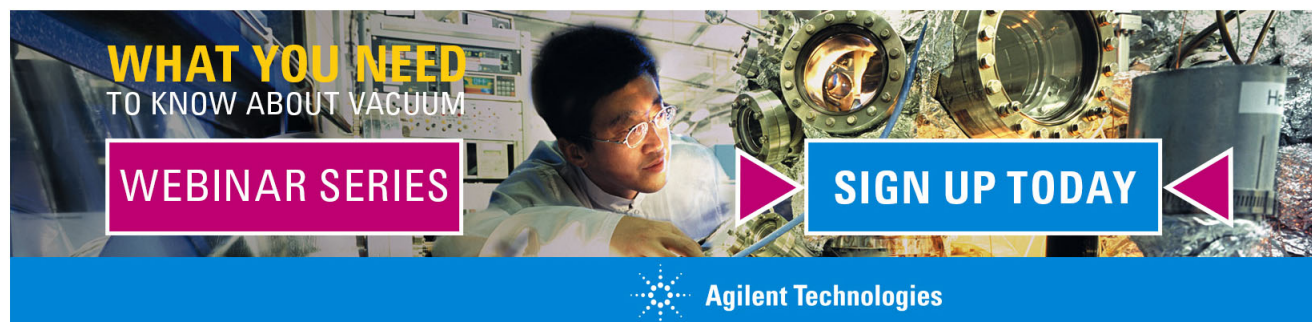
[The role of Au nanorods in highly efficient inverted low bandgap polymer solar cells](#)  
Appl. Phys. Lett. **105**, 223305 (2014); 10.1063/1.4903514

[TiO<sub>x</sub>/Al bilayer as cathode buffer layer for inverted organic solar cell](#)  
Appl. Phys. Lett. **103**, 173303 (2013); 10.1063/1.4826562

[Small molecule solution-processed bulk heterojunction solar cells with inverted structure using porphyrin donor](#)  
Appl. Phys. Lett. **102**, 013305 (2013); 10.1063/1.4773910

[Light-soaking issue in polymer solar cells: Photoinduced energy level alignment at the sol-gel processed metal oxide and indium tin oxide interface](#)  
J. Appl. Phys. **111**, 114511 (2012); 10.1063/1.4728173

---

The advertisement features a background image of a scientist in a lab coat working with a piece of scientific equipment. Overlaid on the image is a yellow banner at the top with the text 'WHAT YOU NEED TO KNOW ABOUT VACUUM' in bold, black, sans-serif font. Below this, there are two buttons: a pink one on the left with the text 'WEBINAR SERIES' in white, and a blue one on the right with the text 'SIGN UP TODAY' in white. The Agilent Technologies logo, which consists of a stylized starburst icon followed by the company name, is positioned at the bottom center of the advertisement.

# Direct observation of UV-induced charge accumulation in inverted-type polymer solar cells with a $\text{TiO}_x$ layer: Microscopic elucidation of the light-soaking phenomenon

D. Son,<sup>1</sup> T. Kuwabara,<sup>2</sup> K. Takahashi,<sup>2</sup> and K. Marumoto<sup>1,3,a)</sup>

<sup>1</sup>Division of Materials Science, University of Tsukuba, Tsukuba, Ibaraki 305-8573, Japan

<sup>2</sup>Graduate School of Natural Science and Technology, Kanazawa University, Kanazawa, Ishikawa 920-1192, Japan

<sup>3</sup>Tsukuba Research Center for Interdisciplinary Materials Science (TIMS), University of Tsukuba, Tsukuba, Ibaraki 305-8573, Japan

(Received 4 March 2016; accepted 11 September 2016; published online 27 September 2016)

The mechanism of light-soaking phenomenon in inverted-type organic solar cells (IOSCs) with a structure of indium-tin-oxide/ $\text{TiO}_x$ /P3HT:PCBM/Au was studied by electron spin resonance (ESR) spectroscopy. Charge accumulation in the cell during UV-light irradiation was observed using ESR, which was clearly correlated with the light-soaking phenomenon. The origin of the charge accumulation is clarified as holes that are deeply trapped at p-type P3HT polymer-chain ends with bromine after hole transfer from the band excitation in the  $\text{TiO}_x$  layer. The holes are considered to be electrostatically attracted to trapped electrons in the  $\text{TiO}_x$  layer after the band excitation. These accumulated charges are the origin of the light-soaking phenomenon. Our results strongly suggest that passivation of the residual OH groups in the  $\text{TiO}_x$  layer is needed to avoid the light-soaking phenomenon by preventing electron trappings, a step that is indispensable in the operation of highly stable IOSCs without UV-light irradiation based on a low-cost and low-temperature device fabrication process using flexible plastic substrates. *Published by AIP Publishing.*

[<http://dx.doi.org/10.1063/1.4963285>]

Inverted-type organic solar cells (IOSCs) represent a promising organic solar cell technology because they are highly stable, have the potential for low-cost fabrication, and can operate in air even without encapsulation of the devices.<sup>1,2</sup> Recently, the power conversion efficiency (PCE) has been greatly improved to more than 10%, which has promoted research and development of the practical use in commercial applications.<sup>3–7</sup> One of the fundamental issues is the light-soaking phenomenon with respect to UV-light irradiation, which has been commonly observed in IOSCs with electron-collecting layers such as  $\text{TiO}_x$ .<sup>2,8–15</sup> Although high-temperature annealing treatments on the  $\text{TiO}_x$  layer can prevent the phenomenon, such treatments are undesirable for low-temperature device fabrication using flexible plastic substrates.<sup>15</sup> Additionally, long-term UV-light irradiation on IOSCs can cause device degradation. Thus, the mechanism of the light-soaking phenomenon must be elucidated to operate IOSCs without UV-light irradiation. Although the light-soaking phenomenon has been explained on the basis of charge-trap fillings in the electron-collecting layers using phenomenological methods, the mechanism is not yet completely understood, and a microscopic investigation using a direct research method is greatly desired.<sup>9–14,16</sup>

To fully elucidate the light-soaking phenomenon, electron spin resonance (ESR) spectroscopy is the most suitable technique because ESR is a highly sensitive and nondestructive technique for directly observing the charges in organic semiconductors and their devices at the molecular level.<sup>17–24</sup> ESR studies have demonstrated a clear correlation between performance deterioration and charge accumulation (or

trappings) in a normal-type OSC,<sup>18</sup> and have clarified degradation mechanism due to charge formation during device fabrication.<sup>19</sup> As noted above, the light-soaking phenomenon has been considered to be related to charge trappings. Thus, ESR is a powerful tool for elucidating the light-soaking phenomenon from a microscopic viewpoint. Organic solar-cell materials, such as polymers and fullerenes, have been studied by ESR.<sup>20–24</sup> However, the ESR study of organic solar cells has not yet been reported except for our studies.<sup>18,19</sup>

Here we study the light-soaking phenomenon of IOSCs with a  $\text{TiO}_x$  electron-collecting layer during device operation using ESR. A direct observation of charge accumulation in the IOSCs and the correlation with the performance improvement under UV-light irradiation are presented. This correlation is an interesting result that is completely different from that for normal-type OSCs.<sup>18</sup> The origin of the charge accumulation is clarified as holes that are deeply trapped at polymer-chain ends with bromine. The holes are considered to be electrostatically attracted to trapped electrons in the  $\text{TiO}_x$  layer. These accumulated charges are the origin of the light-soaking phenomenon.

To attain a high signal-to-noise ratio of the ESR signal by increasing the active area of the device, we utilized a rectangular device structure (3 mm × 20 mm) in an ESR sample tube with an inner diameter of 3.5 mm (see Figure 1(a)).<sup>18,19</sup> The structure is indium-tin-oxide (ITO)/ $\text{TiO}_x$ /poly(3-hexylthiophene) (P3HT):[6,6]-phenyl  $\text{C}_{61}$ -butyric acid methyl ester (PCBM)/Au.<sup>2,15</sup> The  $\text{TiO}_x$  layer (~30 nm) was fabricated by a chemical bath deposition (CBD) method.<sup>2,15</sup> An active P3HT:PCBM layer (~250 nm) was spin-coated on the  $\text{TiO}_x$  layer. An Au hole-collecting electrode (~150 nm) was

<sup>a)</sup>Electronic mail: marumoto@ims.tsukuba.ac.jp

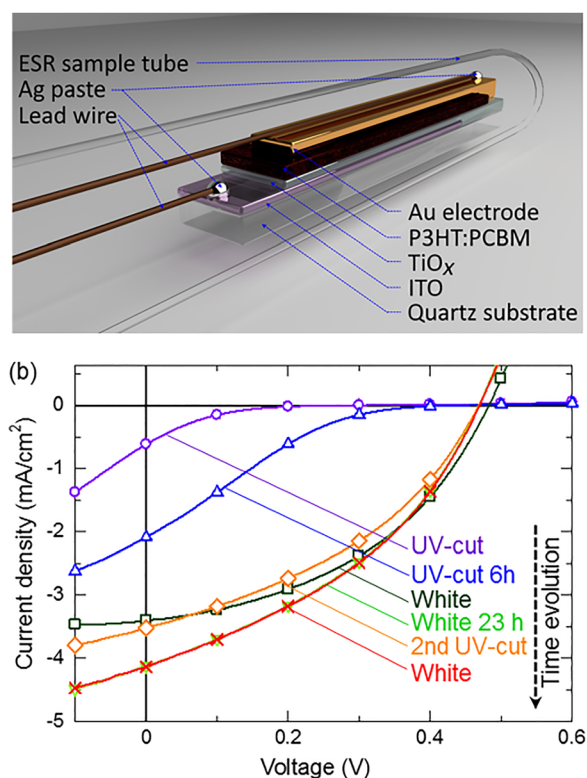


FIG. 1. (a) A schematic device structure of an inverted-type polymer solar cell of indium-tin-oxide (ITO)/TiO<sub>x</sub>/poly(3-hexylthiophene) (P3HT):phenyl C<sub>61</sub>-butyric acid methyl ester (PCBM)/Au for electron spin resonance (ESR) measurements. (b)  $J$ - $V$  characteristics of the device under various light irradiation conditions. The dashed arrow indicates time evolution.

vapor-deposited on the fabricated film. The device was sealed in an ESR sample tube under a nitrogen glove-box atmosphere. The active area was 0.16 cm<sup>2</sup>. Samples for low-temperature measurements were sealed in an ESR sample tube with helium gas at 100 Torr. Further details are provided in [supplementary material](#).

To confirm the light-soaking phenomenon, the current density ( $J$ )-voltage ( $V$ ) characteristics were measured under various light irradiation conditions. In the following, we define the notations “White light” and “UV-cut light” as simulated solar irradiation including and excluding UV-light with a wavelength of <420 nm using a UV-cut filter, respectively. Figure 1(b) exhibits the typical behavior of the light-soaking phenomenon; the  $J$ - $V$  curve remained in an S-shape until the device was irradiated by white light. When the device was irradiated by white light, the cell performance greatly improved, showing a proper J-shaped  $J$ - $V$  curve, and the curve then maintained the J-shape under irradiation of both white light and brief UV-cut light.<sup>8–13,15</sup>

Direct evidence for the light-soaking-induced charge accumulation is demonstrated by ESR measurements. Figures 2(a)–2(d) present ESR signals of the device under short-circuit conditions before and during device operation. In these experiments, a continuous-wave method was used with a modulation frequency of 100 kHz for the external magnetic field  $H$ .<sup>18</sup> Thus, the observed light-induced ESR signals are due to accumulated (or deeply trapped) photogenerated charge carriers with a lifetime of >10  $\mu$ s.<sup>18</sup> The ESR signal can be deconvoluted into two signals with a broad

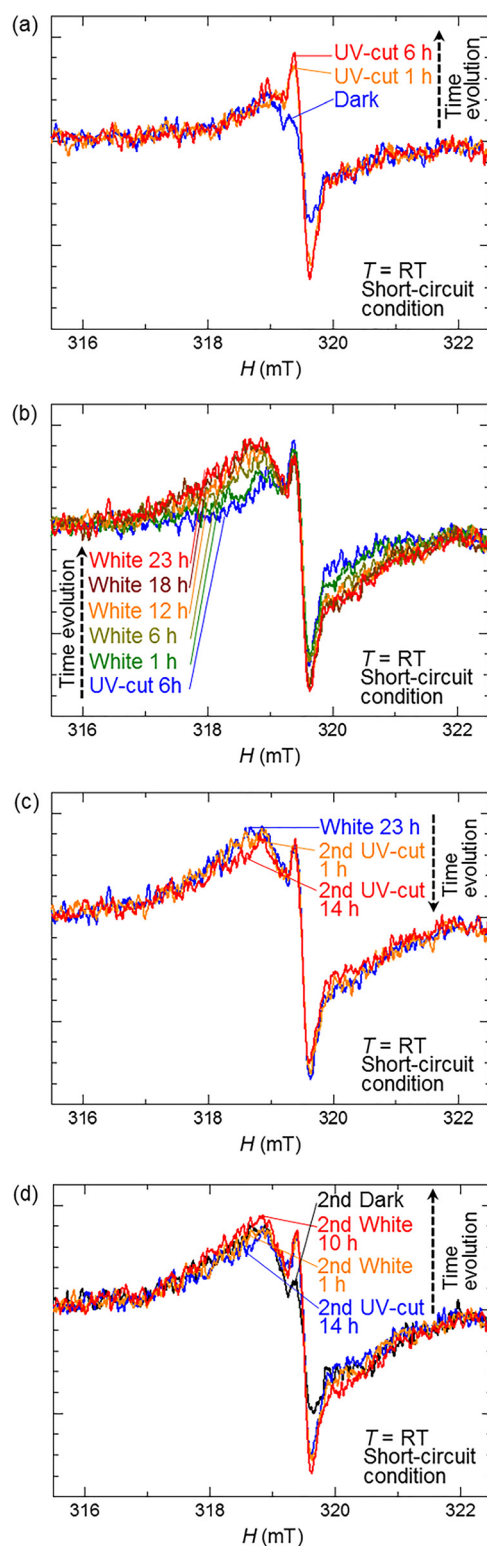


FIG. 2. (a)–(d) ESR signals of short-circuited ITO/TiO<sub>x</sub>/P3HT:PCBM/Au inverted-type polymer solar cells under various light irradiation conditions at room temperature. The dashed arrow indicates time evolution. Each figure shows the ESR spectral change from (a) dark conditions to UV-cut irradiation, (b) UV-cut to white light irradiation, (c) white light to 2nd UV-cut irradiation, and (d) 2nd UV-cut to 2nd white light irradiation and then under 2nd dark conditions.

and narrow linewidth (see Figure 3(a)), which are defined as the broad and narrow components, respectively. The  $g$  value and peak-to-peak ESR linewidth  $\Delta H_{pp}$  of each component were determined as  $g_{broad} = 2.0033$ ,  $\Delta H_{pp} = 0.96$  mT and



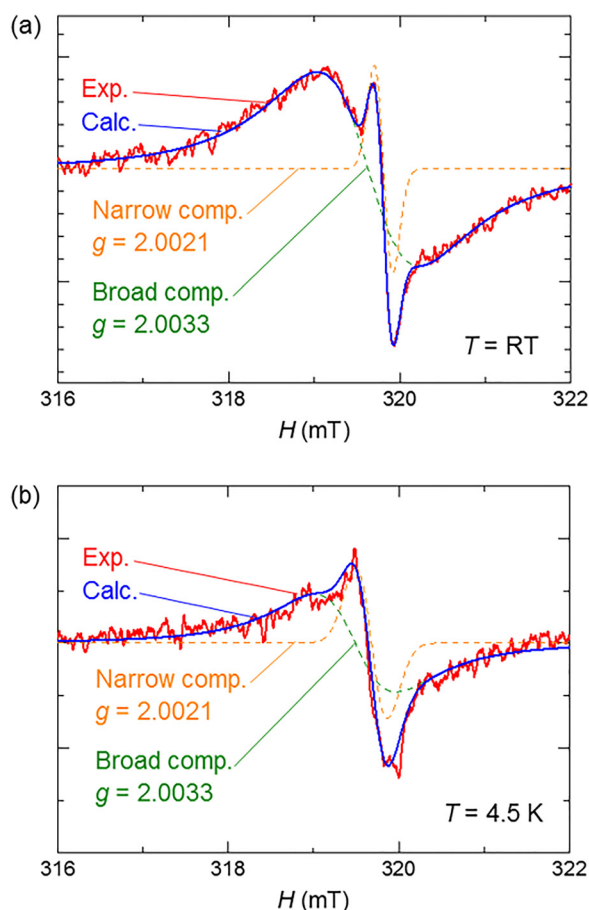


FIG. 3. (a) and (b) Fitting curves with two-component deconvolution to the observed ESR signal for (a) a device subjected to 10 h of 2nd white light irradiation and (b) the ITO/TiO<sub>x</sub>/P3HT sample at 4.5 K, where the  $g$  values of the respective components of the signal were similar to those of the device.

$g_{\text{narrow}} = 2.0021$ ,  $\Delta H_{\text{pp}} = 0.22$  mT, respectively. No anisotropy was observed for the  $H$  direction with respect to the substrate. The narrow component immediately increased under UV-cut light (see Figure 2(a)) and decreased under dark conditions (see Figure 2(d)). The response time could not be determined because the signals were averaged over 1 h. Once the narrow component increased, almost no changes in both components were observed under UV-cut light (see UV-cut 1 h and UV-cut 6 h in Fig. 2(a)). In contrast, the broad component gradually increased under white light (see Figures 2(b) and 2(d)) and decreased under UV-cut light (see Figure 2(c)). Note that the broad component has a strong correlation with UV-light irradiation.

The origins of both components are discussed based on the ESR parameters. The narrow component is identified as the ESR signal of radical cations (positive polarons or holes) in P3HT that were generated by light-induced charge separation in the P3HT:PCBM layer.<sup>18</sup> The averaged  $g$  value ( $g_{\text{narrow}} = 2.0021$ ) is theoretically reproduced by the density functional theory (DFT) calculation for a radical cation of a thiophene hexamer (see Figure S1 and Table S1 of [supplementary material](#)). However, the ESR parameters of the broad component are considerably larger than those of the narrow component. To identify the origin, we measured ESR signals of quartz/TiO<sub>x</sub> and quartz/TiO<sub>x</sub>/P3HT thin-film

samples. The quartz/TiO<sub>x</sub> sample did not show any ESR signal. However, the quartz/TiO<sub>x</sub>/P3HT sample showed an ESR signal similar to that of the device (see Figure 3(b)). Therefore, the origin of the broad component is related to the TiO<sub>x</sub>/P3HT interface. As discussed later, the origin is attributed to accumulated holes at P3HT polymer-chain ends with bromine. Note that PCBM radical anions are undetectable with ESR at room temperature because of their rapid spin relaxation.<sup>18,23</sup> Also, we have confirmed no ESR signal due to accumulated electrons on PCBM in the device under dark conditions at low temperatures below 77 K just after white light irradiation at room temperature.

To clarify the photoresponse of the ESR signal, the transient responses under various light irradiation conditions are discussed. To present the ESR intensity, the number of spins ( $N_{\text{spin}}$ ) was evaluated by integrating the ESR spectrum twice and by comparing the standard Mn<sup>2+</sup> marker sample.<sup>18</sup> Figure 4(a) shows the transient response of the  $N_{\text{spin}}$  upon light irradiation, which exhibits a clear photoresponse. In spite of the relatively large amplitude of the signal, the  $N_{\text{spin}}$  responsible for the narrow component is small, because the amplitude is related to the square of the ESR linewidth; the total  $N_{\text{spin}}$  is primarily attributed to the broad component. The  $N_{\text{spin}}$  due to the narrow component showed little change under both conditions of white light and UV-cut light because the narrow component is caused by the light-induced charge separation in the P3HT:PCBM layer. Its fast photoresponse within 1 h confirms that this component is due to P3HT radical cations with short lifetimes. In contrast, the  $N_{\text{spin}}$  of the broad component gradually increased under white light and decreased under UV-cut light or dark conditions, which was reversible. Therefore, the broad component originates from deeply trapped charges in the device, not from radical species due to decomposed and/or oxidized materials.

The simultaneous measurement of  $N_{\text{spin}}$  and short-circuit current density ( $J_{\text{sc}}$ ) is a powerful way to clarify the correlation between the broad component and the light-soaking phenomenon. Figure 4(b) shows the transient response of total  $N_{\text{spin}}$  and  $J_{\text{sc}}$  using the same device under white light and UV-cut light. The  $N_{\text{spin}}$  behavior is similar to that of Fig. 4(a). The  $N_{\text{spin}}$  and  $J_{\text{sc}}$  rapidly increased immediately after exposure to white light, and then both continued to gradually increase. When exposed to UV-cut light, both  $N_{\text{spin}}$  and  $J_{\text{sc}}$  gradually decreased. These photoresponses demonstrate the clear correlation between the broad component and the light-soaking phenomenon.

We now turn to a discussion of the mechanism of the light-soaking phenomenon. The reason for the larger ESR parameters of the broad component than those of the narrow components is ascribed to hole accumulation at P3HT polymer-chain ends with bromine, as explained below. In the synthesis of P3HT, some of bromines may remain at polymer-chain ends due to an incomplete reaction during polymerization.<sup>25–27</sup> In fact, we have found residual bromine atoms in our P3HT using energy-dispersive X-ray spectroscopy (EDS) measurements (see Figure S2 and Table S4 of [supplementary material](#)). The end groups with bromine have been reported to act as hole-trapping sites.<sup>28</sup> The hole trapping is also supported by the shallower ionization potential

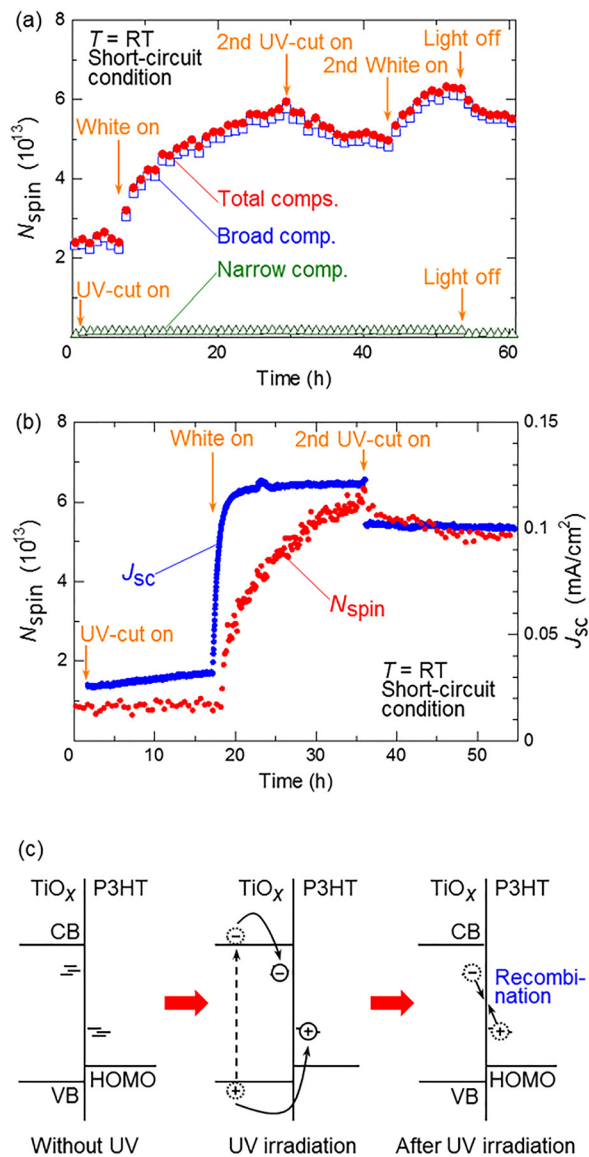


FIG. 4. (a) Transient response of the number of spins ( $N_{\text{spin}}$ ) of an ITO/TiO<sub>x</sub>/P3HT:PCBM/Au cell to UV-cut and white light irradiation. The  $N_{\text{spin}}$  is obtained from the ESR signal averaged over 1 h. (b) Transient response of  $N_{\text{spin}}$  (red circles) and  $J_{\text{sc}}$  (blue circles) of an ITO/TiO<sub>x</sub>/P3HT:PCBM/Au cell to UV-cut and white light irradiation. The  $N_{\text{spin}}$  is obtained from the ESR signal averaged over 30 min. For the measurement, a device was fabricated in the same manner as that for the device shown in Fig. 1. A discontinuous point for  $J_{\text{sc}}$  at approximately 36 h is ascribed to the decrease in light intensity due to the UV-cut filter. (c) Charge trapping scheme with respect to UV-light irradiation.

of 2-bromo thiophene ( $8.664 \pm 0.005$  eV (Ref. 29)) than that of thiophene ( $8.872 \pm 0.005$  eV (Ref. 29) or  $8.87 \pm 0.01$  eV (Ref. 30)); the bromine “lone pair” atomic orbitals considerably participate in the highest occupied molecular orbital (HOMO), which decreases the ionization potential.<sup>29</sup> When holes are trapped at such sites, holes’ spins are affected by nearby heavy-atom bromine via large spin-orbit couplings, resulting in a large  $g$  value. This explanation is fully consistent with the observed larger  $g$  value of the broad component ( $g_{\text{broad}} = 2.0033$ ) than that of the narrow component ( $g_{\text{narrow}} = 2.0021$ ) (see Figures 3(a) and 3(b)). Moreover, the larger  $g$  value is reproduced by DFT calculations for a radical cation of a bromine-monosubstituted 6T (6T-Br) (see Table S1 of supplementary material). Furthermore, the DFT

calculations indicate a larger hyperfine coupling constant at bromine than that at hydrogen, which is due to a larger spin density ( $\sigma$ ) at bromine than that at hydrogen (see Tables S2 and S3 of supplementary material). Large spin density on an atom gives rise to a large hyperfine interaction.<sup>31</sup> The hyperfine interaction with bromine splits one resonance line into four, because natural abundant bromine has a nuclear spin  $I = 3/2$ . This could make ESR linewidth further broader. These effects reasonably explain the broader ESR linewidth ( $\Delta H_{\text{pp}} = 0.96$  mT) than that of the narrow component ( $\Delta H_{\text{pp}} = 0.22$  mT) because the ESR linewidth arises from the hyperfine interactions between the  $\pi$ -electron’s spin and the nuclear spins.<sup>17,31</sup>

On the basis of the increase in the broad component upon UV-light irradiation of  $>2.95$  eV, the source of the accumulated holes is considered to originate from the band excitation in TiO<sub>x</sub> with a bandgap of  $\sim 3.2$  eV. When holes from the band excitation can transfer to P3HT before recombining with their counterpart electrons in TiO<sub>x</sub>, the band excitation can supply holes to trapping sites at the TiO<sub>x</sub>/P3HT interface. The accumulated holes are electrostatically attracted to residual trapped electrons in TiO<sub>x</sub>. Another possible source of holes due to photocurrent generation in the P3HT:PCBM layer is excluded due to the absence of an increase in the broad component under UV-cut light.

The trapping sites for electrons in TiO<sub>x</sub> are discussed here. Ti<sup>4+</sup> ions in anatase-type TiO<sub>2</sub> have been reported to act as electron-trapping sites.<sup>32</sup> When an electron is trapped at such a site forming a Ti<sup>3+</sup> ion, the site becomes ESR-active ( $g \sim 1.9$ ).<sup>32</sup> For the quartz/TiO<sub>x</sub> and quartz/TiO<sub>x</sub>/P3HT samples, however, such an ESR signal was not observed, even at temperatures below 77 K. Thus, Ti<sup>4+</sup> ions do not act as electron-trapping sites. Other possible electron-trapping sites are OH groups in TiO<sub>x</sub>. Many OH groups are residual in TiO<sub>x</sub> film.<sup>33</sup> When an OH group can capture an electron and the capture can weaken the bonding between the OH group and Ti, an ESR-inactive OH<sup>−</sup> ion can be formed.<sup>34</sup> Since the process is reversible, the OH<sup>−</sup> ion may be electrostatically captured nearby Ti, which may be expressed as  $\equiv \text{Ti} - \text{OH} + e^- \rightarrow \equiv \text{Ti} \cdots \text{OH}^-$  where the dotted line “ $\cdots$ ” represents an electrostatic capture. Such electron-trap fillings at OH groups can greatly improve the electron-transport characteristics of the TiO<sub>x</sub> layer. Therefore, from the results of our study we conclude that these electron trappings are the main mechanism of the light-soaking phenomenon.

Figure 4(c) illustrates the charge trapping scheme. Without UV-light irradiation, both electron and hole trapping sites in TiO<sub>x</sub> and P3HT remain unoccupied (Figure 4(c), left-hand side). Once the device is irradiated with UV light, the device performance shows dramatic improvement as both electron and hole trapping sites are filled with band-excited electrons and holes, respectively (Figure 4(c), center). After UV-light irradiation, the trapped electrons and holes slowly recombine, resulting in a gradual decrease in  $J_{\text{sc}}$  (Figure 4(c), right-hand side).

The light-soaking phenomenon is considered to depend on the trapping densities in IOSCs. Thus, it would be an interesting subject to perform ESR experiments on IOSCs where TiO<sub>x</sub> and polymers have different OH-group and bromine content, respectively. Such IOSCs may be fabricated

using different annealing temperatures for  $\text{TiO}_x$  layers, different polymer-molecular weights, polymers with different end-capping, or prepared without the bromine. Further ESR studies for such IOSCs are currently in progress, and will be reported in a separate paper.

Our study elucidates the mechanism of the light-soaking phenomenon in typical IOSCs using ESR spectroscopy. Our method provides direct evidence of UV-induced hole accumulation in IOSCs, and demonstrates a clear correlation with the light-soaking phenomenon. The correlated increase in both ESR and device performance is in clear contrast to the inverse correlation between ESR and performance reported for normal-type OSCs.<sup>18</sup> This interesting observation indicates a larger number of deep trapping sites in IOSCs with a  $\text{TiO}_x$  layer than that in the normal-type OSCs. Our results strongly suggest passivation of the residual OH groups in  $\text{TiO}_x$  to avoid the light-soaking phenomenon by preventing electron trapings, a step that is indispensable in the operation of highly stable IOSCs without UV-light irradiation based on a low-cost and low-temperature device fabrication process using flexible plastic substrates. Although accessible time-scales of our presented experiments are limited to above 10  $\mu\text{s}$  due to the  $H$  modulation frequency of 100 kHz, our method has higher sensitivity for detecting accumulated photogenerated carriers compared with current-detected ESR experiments because the current-detected ESR experiments are not suitable for detecting accumulated carriers. Our method is general and should be applicable to the elucidation of light-soaking phenomena in other solar cells.

See [supplementary material](#) for details of the device fabrication, the DFT calculation, and the EDS measurement on a P3HT powder sample.

We thank Professor Y. Kobori, Professor H. Ohkita, and Dr. Y. Tamai for valuable discussions. This work was partially supported by JSPS KAKENHI (Grant Nos. 24560004 and 15K13329) and by JST, PRESTO.

<sup>1</sup>L. M. Chen, Z. Hong, G. Li, and Y. Yang, *Adv. Mater.* **21**, 1434 (2009).

<sup>2</sup>T. Kuwabara, T. Nakayama, K. Uozumi, T. Yamaguchi, and K. Takahashi, *Sol. Energy Mater. Sol. Cells* **92**, 1476 (2008).

<sup>3</sup>Z. He, C. Zhong, S. Su, M. Xu, H. Wu, and Y. Cao, *Nat. Photonics* **6**, 591 (2012).

<sup>4</sup>A. K. K. Kyaw, D. H. Wang, V. Gupta, J. Zhang, S. Chand, G. C. Bazan, and A. J. Heeger, *Adv. Mater.* **25**, 2397 (2013).

<sup>5</sup>M. Song, J.-W. Kang, D.-H. Kim, J.-D. Kwon, S.-G. Park, S. Nam, S. Jo, S. Y. Ryu, and C. S. Kim, *Appl. Phys. Lett.* **102**, 143303 (2013).

<sup>6</sup>S. Woo, W. H. Kim, H. Kim, Y. Yi, H.-K. Lyu, and Y. Kim, *Adv. Energy Mater.* **4**, 1301692 (2014).

<sup>7</sup>V. Vohra, K. Kawashima, T. Kakara, T. Koganezawa, I. Osaka, K. Takimiya, and H. Murata, *Nat. Photonics* **9**, 403 (2015).

<sup>8</sup>H. Schmidt, K. Zilberberg, S. Schmale, H. Flugge, T. Riedl, and W. Kowalsky, *Appl. Phys. Lett.* **96**, 243305 (2010).

<sup>9</sup>J. Kim, G. Kim, Y. Choi, J. Lee, S. H. Park, and K. Lee, *J. Appl. Phys.* **111**, 114511 (2012).

<sup>10</sup>S. Chambon, E. Destouesse, B. Pavageau, L. Hirsch, and G. Wantz, *J. Appl. Phys.* **112**, 094503 (2012).

<sup>11</sup>Z. Lin, C. Jiang, C. Zhu, and J. Zhang, *ACS Appl. Mater. Interfaces* **5**, 713 (2013).

<sup>12</sup>S. Trost, K. Zilberberg, A. Behrendt, A. Polywka, P. Gorn, P. Reckers, J. Maibach, T. Mayer, and T. Riedl, *Adv. Energy Mater.* **3**, 1437 (2013).

<sup>13</sup>F. J. Lim, Y. T. Set, A. Krishnamoorthy, J. Ouyang, J. Luther, and G. W. Ho, *J. Mater. Chem. A* **3**, 314 (2015).

<sup>14</sup>S. Trost, T. Becker, K. Zilberberg, A. Behrendt, A. Polywka, R. Heiderhoff, P. Gorn, and T. Riedl, *Sci. Rep.* **5**, 7765 (2015).

<sup>15</sup>T. Kuwabara, K. Yano, T. Yamaguchi, T. Taima, K. Takahashi, D. Son, and K. Marumoto, *J. Phys. Chem. C* **119**, 5274 (2015).

<sup>16</sup>C. S. Kim, S. S. Lee, E. D. Gomez, J. B. Kim, and Y.-L. Loo, *Appl. Phys. Lett.* **94**, 113302 (2009).

<sup>17</sup>K. Marumoto, S. Kuroda, T. Takenobu, and Y. Iwasa, *Phys. Rev. Lett.* **97**, 256603 (2006).

<sup>18</sup>T. Nagamori and K. Marumoto, *Adv. Mater.* **25**, 2362 (2013).

<sup>19</sup>K. Marumoto, T. Fujimori, M. Ito, and T. Mori, *Adv. Energy Mater.* **2**, 591 (2012).

<sup>20</sup>J. De Ceuster, E. Goovaerts, A. Bouwen, J. C. Hummelen, and V. Dyakonov, *Phys. Rev. B* **64**, 195206 (2001).

<sup>21</sup>N. A. Schultz, M. C. Scharber, C. J. Brabec, and N. S. Sariciftci, *Phys. Rev. B* **64**, 245210 (2001).

<sup>22</sup>O. G. Poluektov, S. Filippone, N. Martín, A. Sperlich, C. Deibel, and V. Dyakonov, *J. Phys. Chem. B* **114**, 14426 (2010).

<sup>23</sup>A. Aguirre, S. C. J. Meskers, R. A. J. Janssen, and H.-J. Egelhaaf, *Org. Electron.* **12**, 1657 (2011).

<sup>24</sup>J. Niklas, K. L. Mardis, B. P. Banks, G. M. Grooms, A. Sperlich, V. Dyakonov, S. Beaupré, M. Leclerc, T. Xu, L. Yu, and O. G. Poluektov, *Phys. Chem. Chem. Phys.* **15**, 9562 (2013).

<sup>25</sup>R. D. McCullough, S. Tristram-Nagle, S. P. Williams, R. D. Lowe, and M. Jayaraman, *J. Am. Chem. Soc.* **115**, 4910 (1993).

<sup>26</sup>T.-A. Chen, X. Wu, and R. D. Rieke, *J. Am. Chem. Soc.* **117**, 233 (1995).

<sup>27</sup>R. S. Loewe, S. M. Khersonsky, and R. D. McCullough, *Adv. Mater.* **11**, 250 (1999).

<sup>28</sup>Y. Kim, S. Cook, J. Kirkpatrick, J. Nelson, J. R. Durrant, D. D. C. Bradley, M. Giles, M. Heeney, R. Hamilton, and I. McCulloch, *J. Phys. Chem. C* **111**, 8137 (2007).

<sup>29</sup>J. W. Rabalais, L. O. Werme, T. Bergmark, L. Karlsson, and K. Siegbahn, *Int. J. Mass Spectrom. Ion Phys.* **9**, 185 (1972).

<sup>30</sup>J. J. Butler and T. Baer, *J. Am. Chem. Soc.* **102**, 6764 (1980).

<sup>31</sup>D. Son, K. Marumoto, T. Kizuka, and Y. Shimoi, *Synth. Met.* **162**, 2451 (2012).

<sup>32</sup>M. Chiesa, M. C. Paganini, S. Livraghi, and E. Giamello, *Phys. Chem. Chem. Phys.* **15**, 9435 (2013).

<sup>33</sup>T. Kuwabara, H. Sugiyama, M. Kuzuba, T. Yamaguchi, and K. Takahashi, *Org. Electron.* **11**, 1136 (2010).

<sup>34</sup>L.-L. Chua, J. Zaumseil, J.-F. Chang, E. C.-W. Ou, P. K.-H. Ho, H. Sirringhaus, and R. H. Friend, *Nature* **434**, 194 (2005).